M Star Astrosphere Size Fluctuations and Habitable Planet Descreening*

David S. Smith† and John M. Scalo

Department of Astronomy, The University of Texas at Austin, Austin, TX 78712

June 9, 2009

Keywords: Habitable planets; habitable zones; M stars; extrasolar planets; astrospheres; heliospheres

Abstract

Stellar astrospheres—the plasma cocoons carved out of the interstellar medium by stellar winds—are continually influenced by their passage through the fluctuating interstellar medium (ISM). Inside dense interstellar regions, an astrosphere may be compressed to a size smaller than the liquid-water habitable zone distance. Habitable planets then enjoy no astrospheric buffering from the full flux of Galactic cosmic rays and interstellar dust and gas, a situation we call "descreening." Recent papers (Yeghikyan and Fahr, Pavlov *et al*.) have suggested such global consequences as severe ozone depletion and glaciation. Using a ram-pressure balance model that includes gravitational focusing of the interstellar flow, we compute the size of the astrosphere in the apex direction as a function of parent star mass. We derive a dependence on the parent-star mass M due to gravitational focusing for densities larger than about 100 $(M/M_{\odot})^{-2}$ cm^{-3}. We calculate the interstellar densities required to descreen planets in the habitable zone of solar- and subsolar-mass stars and find a critical descreening density of roughly 600 $(M/M_{\odot})^{-2}$ cm^{-3} for the Sun's velocity relative to the local ISM. Finally, we estimate from ISM observations the frequency of descreening encounters as 1–10 Gyr^{-1} for solar-type stars and 10^2–10^9 times smaller for M

*To be published in *Astrobiology*

†Corresponding author: dss@lpl.arizona.edu; Present affiliation: Lunar and Planetary Laboratory, University of Arizona, Tucson, AZ 85721

stars. Given this disparity, we conclude that M star habitable-zone planets are virtually never exposed to the severe effects discussed by Yeghikyan and Fahr and Pavlov *et al*.

1 Introduction

The heliosphere is the magnetic bubble carved out of the interstellar medium by the expanding solar wind. A recurring idea is that during the Sun's lifetime encounters with dense interstellar environments have compressed the heliosphere, enhancing cosmic ray fluxes and hydrogen accretion, affecting atmospheric chemistry (including ozone), and perhaps altering surface mutation rates and climate (e.g. Fahr, 1968; McCrea, 1975; Talbot *et al*., 1976; Begelman and Rees, 1976; Talbot and Newman, 1977; McKay and Thomas, 1978; Yabushita and Allen, 1989; Bzowski *et al*., 1996; Zank and Frisch, 1999; Scherer *et al*., 2002; Florinski *et al*., 2003; Yeghikyan and Fahr, 2004a,b; Pavlov *et al*., 2005a,b; Frisch and Slavin, 2006; Müller et al., 2006; Zank et al., 2006; Müller et al., 2008). There may even be empirical evidence for such an encounter in lunar soil samples (Wimmer-Schweingruber and Bochsler, 2000, 2001). A similar variation should appear for other stars, given that "astrospheres" around other stars have now been directly observed through their interaction with the interstellar medium (Wood *et al*., 2002, 2005).

Interest in the potential habitability of planets orbiting stars of mass smaller than the Sun's—cool, red, faint stars of spectral class M with masses between 0.08 and 0.6 $M_{\odot}$—has increased in recent years. For simplicity, we refer to all subsolar-mass stars as M stars, since K main-sequence stars cover such a small range in mass. The liquid-water habitable zone (HZ) is defined essentially by a certain range in received flux at a planet's surface (Kasting *et al*., 1993), and M star planets have small luminosities, so the habitable-zone distance $r_{\rm HZ}$ can be extremely small, from 0.3 AU to 0.02 AU as mass varies from 0.6 to 0.08 $M_{\odot}$. Habitable planets around M stars may be common for many reasons, including the large number of M stars compared to any other class of star, the detection of extrasolar planets orbiting M stars, their presumed ability to form terrestrial-mass planets if they have sufficiently massive disks, their observed disk frequency, and even evidence for debris disk substructure in one case. See Scalo *et al*. (2007) and Tarter *et al*. (2007) for detailed reviews of these concepts.

The character of the astrospheric environment expected for habitable-zone planets orbiting stars of different masses has not been examined. The present work focuses on the frequency of reductions in the size of a star's astrosphere to within

the HZ or smaller induced by passage through the fluctuating conditions in our Galaxy's interstellar medium (ISM). Such astrosphere size changes are inevitable given the range of conditions in the ISM and may result in significant changes in the Galactic cosmic ray (GCR) flux, as scattering of cosmic rays in the astrosphere is the main filter (besides any possible planetary magnetosphere) shielding planets from GCRs. The effects of GCRs on planetary atmospheres are significant and varied (e.g. Griessmeier *et al*., 2005; Grenfell *et al*., 2006). In addition, changes in astrosphere size should lead to large variations in the planetary accretion rate of interstellar hydrogen or dust, a possibility that has been discussed for several decades (Fahr, 1968; McCrea, 1975; Bzowski *et al*., 1996; Yabushita and Allen, 1989; Florinski *et al*., 2003; Yeghikyan and Fahr, 2004b; Pavlov *et al*., 2005b); the climatic changes associated with such accretion could be varied and severe (e.g. the noctilucent cloud scenario of McKay and Thomas 1978; McKay 1985, or ozone depletion as in Yeghikyan and Fahr 2004b; Pavlov *et al*. 2005b).

In the present paper we show that the size of astrospheres around M stars will be controlled by the star's gravity during descreening episodes and estimate the frequency of these episodes for M stars as compared to solar-type stars. Section 2 will describe the analytic models for astrospheres that we will use, Section 3 gives the resulting mass and age dependences, and Section 3.3 will use these models to estimate the frequency of descreening encounters for solar- and subsolar-mass stars.

2 Methods

2.1 Astrosphere Model

Parker (1963) showed that the location of the termination shock of the solar wind given by the shock-jump conditions was roughly where the ram pressure of the outflowing solar wind balanced the pressure of the counterstreaming ISM:

$$P_{\rm ISM} = \frac{\rho_0 v_0^2 r_0^2}{r_s^2}, \tag{1}$$

where r_s is the termination shock distance, r_0 is a reference distance, ρ_0 is the solar wind mass density at r_0, v_0 is the solar wind velocity at r_0, and $P_{\rm ISM}$ is the total pressure of the ISM, including ram, thermal, and magnetic pressures. When the ISM is streaming supersonically and superalfvenically past the stellar system (such as for the present day solar system), its ram pressure dominates

$P_{\rm ISM}$, such that $P_{\rm ISM} \simeq \rho_{\rm ISM} V^2$, where $\rho_{\rm ISM}$ is the total ISM density and V is the relative velocity between the star and the local ISM flow. Taking the size of the astrosphere r_a to be the distance from the star to the termination shock, we have

$$\frac{r_a}{r_0} = \left(\frac{n_0}{N}\right)^{1/2} \frac{v_0}{V}, \tag{2}$$

where n and N will henceforth refer to the total ion number density of the solar wind and ISM, respectively.

To estimate the stellar wind pressure we assume that the wind within astrospheres of stars of different spectral types (or equivalently masses) are analogues of the solar wind. Little information on the wind is available for stars besides the Sun other than the variation of mass-loss rate with age and type for a few nearby stars (Wood *et al*., 2002, 2005). The wind speed v_0 in our model is taken to be 400 km s^{-1} and assumed to be independent of distance from the star, as is roughly the case for the solar wind in the ecliptic plane (Whang *et al*., 2003) at radii beyond a few times the critical point ($\sim$ 0.1 AU). Recent work suggests that the steady-state wind may in fact be slower and even subsonic and subalfvenic near to the star (Erkaev *et al*., 2005; Preusse *et al*., 2005), in which case the interstellar ram pressure would be balanced by wind magnetic and thermal pressure near M star HZs. Khodachenko *et al*. (2006), however, shows that the steadily higher coronal mass ejection rate on M stars may significantly affect the wind speed in the HZ. To examine the possibility of a slow wind near the HZs of the lowest mass stars, we include a model in our results in which the wind speed is taken to be 50 km s^{-1} instead of 400 km s^{-1}.

For simplicity, we lump the wind density and velocity dependence on stellar mass and age into a scaling function:

$$\xi(M,t) = \left(\frac{M}{M_\odot}\right)^{\alpha} \left(\frac{t}{4.5\ {\rm Gyr}}\right)^{\beta}, \tag{3}$$

where α and β are allowed to vary. Thus the ram pressure balance equation for the astrosphere size can be written:

$$\frac{r_a}{r_0} = \left[\xi(M,t)\frac{n_0}{N}\right]^{1/2} \frac{v_0}{V}. \tag{4}$$

The indices α and β are extremely uncertain as present, but studies of stellar mass loss by Wood *et al*. (2002, 2005) suggest that younger and lower-mass stars may have stronger winds, implying $\alpha \leq 0$ and $\beta \leq 0$.

Observations of Wood *et al*. (2005) suggest $\beta = -2.33$, but, using the same relation between mass-loss rate and X-ray flux as Wood *et al*. (2005), the recent surveys of X-ray fluxes of dwarf M stars by Penz and Micela (2008) suggest $\beta = -1.8$. The mass dependence of the mass-loss rate is more complicated, however, and observations of some M stars show a *lower* mass-loss rate than the Sun (Wood *et al*., 2005). If this is accurate, then it may be possible for M stars to have a lower mass-loss rate than the Sun, in which case, they would be easier to descreen. We include this possibility in our results in an example in which $\alpha = 1$.

Though crude, a pure ram pressure balance approximation is surprisingly accurate at predicting the solar wind termination shock distance and generally yields heliosphere sizes in the apex direction within 10–20% of detailed multifluid, multidimensional computational models (e.g. Zank and Frisch, 1999; Fahr *et al*., 2000; Wood *et al*., 2002; Florinski *et al*., 2004; Zank et al., 2006; Müller et al., 2008). The obvious weakness of this analytic model is that, being one-dimensional, it cannot reproduce the full three-dimensional structure of the global heliosphere. It can, however, predict the minimum ISM densities above which planets in the HZ can be descreened for at least part of their orbit. In one sense, this model may even overestimate the astrosphere size and hence the descreening frequency because it neglects charge exchange with interstellar neutrals.

We have up to now ignored the thermal and magnetic pressure contributions in the ISM. Thermal pressure would be important (for the solar velocity with respect to the local standard of rest) for ISM densities below about 0.1 cm^{-3}, where temperatures are high, but we are interested in the high densities that could lead to descreening, and these regions are typically cold ($T \sim$ 10–20 K, Ferrière, 2001) compared to stellar velocities. For thermal pressure to dominate to ram pressure, the following inequality must be satisfied:

$$T \gtrsim 3000 \left(\frac{V}{10 \text{ km s}^{-1}} \right)^2 \text{ K}, \tag{5}$$

where V is the star-ISM relative velocity. For the Sun, $V = 26$ km s^{-1}, so it would need to enter a region with $T \gtrsim$ 20,000 K for the thermal pressure to compare to the ram pressure in determining the heliosphere size, and these regions usually have densities well below the regimes we are considering here. For instance, the warm ISM has a density below ~ 0.5 cm^{-3} and $T \gtrsim 6000$ K (Ferrière, 2001).

Magnetic pressure is likely to be more important, although without a detailed MHD simulation of the entire ISM structure spanning orders of magnitude in scale, we can make only a rough estimate of the effect. Zeeman observations

(Crutcher, 1999; Bourke *et al*., 2001) can be expressed in the form of an upper limit to a *B*-density relation:

$$B(N) = \begin{cases} 3\ \mu\mathrm{G} & : \quad N < 10\ \mathrm{cm}^{-3} \\ 3\ \left(\frac{N}{10\ \mathrm{cm}^{-3}}\right)^{1/2}\ \mu\mathrm{G} & : \quad N \geq 10\ \mathrm{cm}^{-3} \end{cases} . \tag{6}$$

At densities below 10 cm^{-3} this simply gives a constant pressure $B^2/8\pi$ equal to 4×10^{-13} dyne cm^{-2}. Since the ram pressure is $8 \times 10^{-12}\ NV_{20}^2$ dyne cm^{-2}, the magnetic field isn't competitive with ram pressure until densities below 0.05 cm^{-3} (e.g. in the Local Interstellar Cloud; Florinski *et al*. 2004 have suggested that the magnetic field is anomalously large here). At higher densities, the square-root scaling gives a pressure that is proportional to the density, similar to the ram pressure. In this case the coefficient of the magnetic pressure acts to effectively increase the ISM-star velocity in the ram pressure, but the effect is small, even after multiplying by a small factor (Crutcher, 1999) to statistically account for the fact that only the line-of-sight component of *B* is detected by the Zeeman effect. This is because typical star-ISM velocities exceed the root-mean-square turbulent velocity in the ISM, which is in rough equipartition with the magnetic field. Given these considerations, we neglect the magnetic field for simplicity, with the understanding that we somewhat overestimate the size of the heliosphere at low densities, and that in more realistic ISM models the magnetic field will undergo large fluctuations, often uncorrelated with density, that may lead to episodes of magnetically controlled astrosphere sizes.

2.2 Gravitational Focusing of the Interstellar Flow

As planetary systems traverse dense clouds, gravitational focusing will determine inflowing particle trajectories. This was first pointed out by Fahr (1968) for the case of collisionless orbits of protons in the inner solar system and then later first applied in the present context by Begelman and Rees (1976). Previous work has either neglected gravitational focusing or included its effect on the star-ISM velocity but only in the fluid limit (e.g. Talbot *et al*., 1976; Talbot and Newman, 1977).

Here we assume the ISM flow is collisionless. The mean free path for Coulomb collisions is $\sim 10^{16}\ N^{-1}$ cm, where N is the local ISM number density, and this is larger than the astrosphere size in most cases of interest. This assumption is marginal at low densities, but at the high densities required for descreening,

where gravitational focusing dominates the accretion, we show below that the astrosphere size decreases with ISM density faster than does the collisional mean free path, so the collisionless assumption is valid.

Neglecting collisions simply means that we neglect fluid effects, such as gas pressure, and assume the ISM particles follow ballistic trajectories until they "collide" with the wind-ISM interface, exerting a pressure. The physics of this interaction is beyond the scope of this discussion, but ram-pressure balance approximates the standoff distance between the wind and ISM quite well, and this is our primary concern.

A complete solution to stellar accretion in the collisionless limit was derived by Danby and Camm (1957). The infall density can be expressed as an integral that must be evaluated numerically in the general case, but for our assumption of small gas thermal velocity dispersion, Danby and Camm find that the density in the apex direction is

$$N = N_0 \frac{(q^2 + 2p^2)}{2p(q^2 + p^2)^{1/2}}, \tag{7}$$

where N_0 is the unperturbed ISM number density far from the star, $p \equiv V/\sigma$, $q^2 \equiv 2GM/\sigma^2 r$, and σ is the thermal velocity dispersion of the gas. The ram pressure on the astrosphere in the apex direction will then be this density multiplied by

$$V'^2 = V^2 + \frac{2GM}{r}, \tag{8}$$

where the second term on the right accounts for gravitational acceleration. Balancing the outward wind ram pressure with the inward ISM ram pressure as before yields a quartic polynomial for the astrosphere size r_a (see §3.2). Most of the mass dependence of our result comes from the importance of the gravitational focusing terms involving q^2 in Eq. 7.

3 Results

3.1 Descreening in the High-density Limit

The minimum cloud density N_f for focusing to dominate can be obtained from the condition $b > r_a$, where $b \equiv 2GM/V^2$ is the distance at which the star's gravity becomes important, and r_a is the pressure-balance astrosphere size neglecting

focusing. This gives

$$N_f = 140\ \xi(M,t)\ V_{20}^2\ \left(\frac{M}{M_\odot}\right)^{-2}\ \mathrm{cm}^{-3}, \tag{9}$$

where V_{20} is V in units of 20 km s^{-1}. Thus in dense molecular clouds ($N \sim 10^2$–10^3 or larger; e.g. Larson, 1981; Scalo, 1985) the accretion flow will be mostly determined by gravitational focusing except possibly for the very lowest-mass stars. For reference, the Sun's present speed relative to the local ISM flow is about 26 km s^{-1} (Witte, 2004).

Assuming that gravitational focusing dominates, the density at the apex of the astrosphere is

$$N \simeq \frac{N_0}{2V}\left(\frac{2GM}{r}\right)^{1/2}, \tag{10}$$

where N_0 is the ISM density unperturbed by the star's gravity. The incoming velocity (much larger than the star-gas velocity V in this limit) is $V' \simeq (2GM/r)^{1/2}$. Expressed in terms of the gravitational radius b, we get

$$N \simeq \frac{N_0}{2}\left(\frac{b}{r}\right)^{1/2} \tag{11}$$

and

$$V' \simeq V\left(\frac{b}{r}\right)^{1/2}, \tag{12}$$

where $b/r \gg 1$ in the gravitational focusing limit. Equating NV'^2 to the stellar wind ram pressure then allows a simple solution for the astrosphere size of a planetary system when the flow outside the astrosphere is dominated by gravitational focusing. The result is

$$\frac{r_a}{r_0} \simeq 4\left[\frac{N_0}{\xi(M,t)n_0}\right]^{-2}\left(\frac{V}{v_0}\right)^{-4}\left(\frac{r_0}{b}\right)^3, \tag{13}$$

or, substituting for b,

$$\frac{r_a}{r_0} \simeq \frac{V^2 v_0^4 r_0^3}{2G^3M^3}\left[\frac{N_0}{\xi(M,t)\,n_0}\right]^{-2}. \tag{14}$$

Notice that in this gravitational focusing limit the astrosphere size *increases* with increasing stellar velocity V. This unexpected behavior occurs because the slower

the star is moving, the stronger is the effect of focusing, so that the ram pressure in this case scales like V^{-4}. And since the astrosphere size varies as N_0^{-2} in this limit, while the mean free path of the incoming gas to particle-particle collisions still scales linearly with N_0^{-1}, the astrosphere size is decreasing faster (due to focusing) than the mean free path is, and the validity of the collisionless approximation, as measured by the ratio of mean free path to heliosphere size, *increases* with increasing density. Finally, the inverse mass dependence of the astrosphere size means that the collisionless limit becomes rapidly more accurate for lower mass stars.

By the definition of the HZ (neglecting albedo variations), $r_{\rm HZ} = (L/L_\odot)^{1/2}$ AU where $L_\odot$ is the bolometric luminosity of the Sun. Although no single power law can accurately represent the mass-luminosity relation for low-mass stars (see below), an adequate relation for our purposes is $L/L_\odot = (M/M_\odot)^\alpha$, with $\alpha \sim$ 2–3 for masses between 0.1 and 1 $M_\odot$, based on masses from suitable binary systems (Henry *et al*., 1999; Delfosse *et al*., 2000), Hipparcos distances, and empirical bolometric corrections. The habitable-zone distance is then $r_{\rm HZ} = (M/M_\odot)^{\alpha/2}$ AU. Taking $r_0 = 1$ AU and the average number density of the solar wind at 1 AU, n_0, to be 7 cm^{-3} and evaluating numerical factors:

$$\frac{r_a}{r_{\rm HZ}} \simeq 3.6 \times 10^5 \, \frac{V_{20}^2 \, [\xi(M,t)]^2}{N_0^2} \left(\frac{M}{M_\odot} \right)^{-3-\alpha/2} . \tag{15}$$

The minimum ISM density for this descreening condition to hold is

$$N_d \gtrsim 600 \, V_{20} \, \xi(M,t) \left(\frac{M}{M_\odot} \right)^{-3/2-\alpha/4} {\rm cm}^{-3}, \tag{16}$$

where the numerical coefficient is approximate because the star-gas relative velocity will vary from star to star by factors of a few. For $\alpha = 2.5$, the exponent of M is -2.1, so a star with $M = 0.5 M_\odot$ (early M star) will require an ISM density 4 times larger than the Earth for complete descreening to occur, while a $0.1 M_\odot$ star will require a density about 120 times larger. Our charge exchange model would yield an astrosphere a factor of $(v_0/V)^{1/2}$ smaller for a given ISM density, so it would yield a descreening density that is $(v_0/V)^{1/4}$ times smaller than what the ram pressure approach above would yield. For any reasonable wind speed and ISM-star relative velocity, this would be only a factor of 2–3 at most.

This result is easily understood as a combination of several effects. First, the smaller stellar mass produces less gravitational focusing, reducing the exterior

ram pressure and increasing the astrosphere size compared to larger masses. Second, the habitable-zone distance decreases with decreasing stellar mass, forcing the astrosphere to shrink to smaller distances for descreening of habitable planets to occur. Third, the mass- and age-dependent wind scaling factor $\xi(M,t)$ at a given age probably will increase with decreasing mass, leading to a stronger wind and larger astrosphere.

So far we have assumed the limiting case in which the density field is completely dominated by gravitational focusing in order to get an analytic result. In the following section, we solve the full quartic polynomial equation for the density and give the exact (in the limit of a cold ISM) solution for $r_a/r_{\rm HZ}$ and the critical density for descreening.

3.2 Descreening in the General Case

Following the notation of the previous section, the full polynomial equation for the astrosphere size can be derived in the collisionless limit by equating the wind ram pressure with the ISM ram pressure, using the Danby and Camm (1957) gravitational focusing solution for the density at the astrospheric apex point and the velocity as modified by gravitational focusing (Eq. 8). The result is

$$r_a^4 + 2\,b\,r_a^3 + \frac{5}{4}b^2 r_a^2 + \frac{1}{4}b^3 r_a - \left[\frac{P_w(M,t)}{NV^2}\right]^2 = 0, \tag{17}$$

where b is the gravitational radius as defined earlier and $P_w(M,t) \equiv \xi(M,t)\,n_0 v_0^2 r_0^2$. To solve this equation, first make the substitution $r_a \equiv u - b/2$. This results in the depressed quartic equation:

$$u^4 - \frac{b^2}{4}u^2 - \left[\frac{P_w(M,t)}{NV^2}\right]^2 = 0. \tag{18}$$

Solving for u^2 and taking the positive, real root as the astrosphere size:

$$r_a = \left(\frac{b^2}{8} + \frac{1}{8}\left\{b^4 + \left[\frac{8P_w(M,t)}{NV^2}\right]^2\right\}^{1/2}\right)^{1/2} - \frac{b}{2}. \tag{19}$$

The quantity $r_a/r_{\rm HZ}$ as a function of local ISM density is shown for three representative stellar masses (0.1, 0.5, and 1 $M_\odot$) in Fig. 1.

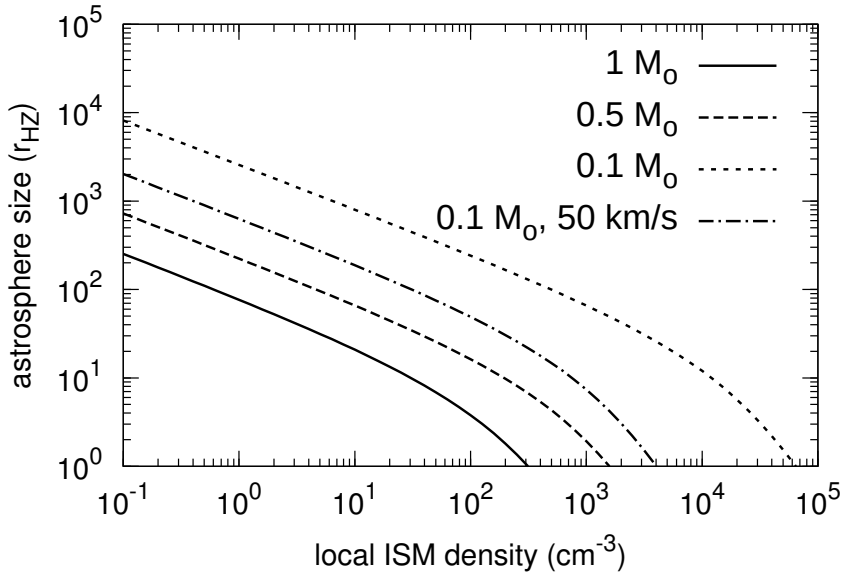

Figure 1: Astrosphere size, in units of liquid-water habitable-zone distance (defined here as the distance receiving the same bolometric stellar flux as Earth), as a function of ambient interstellar gas density for stars of three different masses. The regime in which the inflowing interstellar ram pressure is dominated by gravitational focusing is at densities higher than the "knee" in each curve. The star-ISM relative velocity was taken to be 10 km s^{-1}. The stellar wind speed was taken to be 400 km^{-1} in the first three cases and 50 km s^{-1} in the last case, representing the possibility of subsonic, subalfvenic winds in the HZ of M stars (Erkaev *et al*., 2005; Preusse *et al*., 2005). A slower wind speed seems to have a significant effect on the astrosphere size, but even in this extreme case the astrosphere size is larger for the M star than for a typical solar-mass star for all ISM densities.

Figure 1 shows that the astrosphere is much farther away in terms of the habitable-zone distance $r_{\rm HZ}$ for systems with lower-mass parent stars. The transition into the gravitationally dominated regime is located, for each of the four model planetary systems, by the knee in the curves as the ISM density increases. This knee occurs for lower ISM densities for systems with more massive parent stars, since the effect of the star's gravity on the pressure balance grows at a given ISM density as mass increases. One case is shown with a slow, 50 km^{-1}, wind velocity. This case shows that if M stars do have weaker winds than solar-type stars, then they will have correspondingly smaller astrosphere sizes. But even in the severe case of a wind speed of 50 km $^{-1}$ shown in Fig. 1, the astrosphere is still larger relative to the HZ distance than for the solar-type stars.

Figure 1 also shows clearly that an M star must encounter a very high density interstellar region in order to compress its astrosphere significantly, and therefore full exposures to the Galactic cosmic ray and accretion flux will be rare compared to a solar-type star. This occurs because denser interstellar regions occupy a smaller volume fraction of the Galaxy than lower-density regions, as discussed in §3.3.

A more quantitative calculation of the effect of stellar mass on the critical descreening density is obtained by solving for the density at which the astrosphere apex distance shrinks to the habitable-zone distance $r_{\rm HZ}$, and then relating $r_{\rm HZ}$ to the stellar mass. From Eq. 17 the critical descreening density is

$$N_d = \frac{P_w(M,t)}{V^2}\left(r_{\rm HZ}^4 + 2\,b\,r_{\rm HZ}^3 + \frac{5}{4}\,b^2 r_{\rm HZ}^2 + \frac{1}{4}\,b^3 r_{\rm HZ}\right)^{-1/2}. \qquad (20)$$

The habitable-zone distance depends on the luminosity of the parent star, $r_{\rm HZ} \sim L^{1/2}$ in Earth-Sun units (again ignoring variations in albedo). Because the primary (approximately constant) quantity that governs the evolution of the star is its mass, it is traditional to parameterize L in terms of stellar mass M. We used the data for stellar masses and luminosities for stars less massive than 1 $M_\odot$ given in Hillenbrand and White (2004) and fit the following polynomial to it:

$$\log L = 4.10\log^3 M + 8.16\log^2 M + 7.11\log M + 0.065, \qquad (21)$$

where L and M are in solar units. The slope of this log-log relation varies from about 2 at the smallest masses to about 3 at 0.5–1 $M_\odot$. This allows us to calculate the critical descreening density (Eq. 20) in terms of the parent star mass. The result is plotted for three different mass dependences of $\xi(M,t)$ in Fig. 2 and for an assumed star-ISM velocity of 26 km s^{-1}.

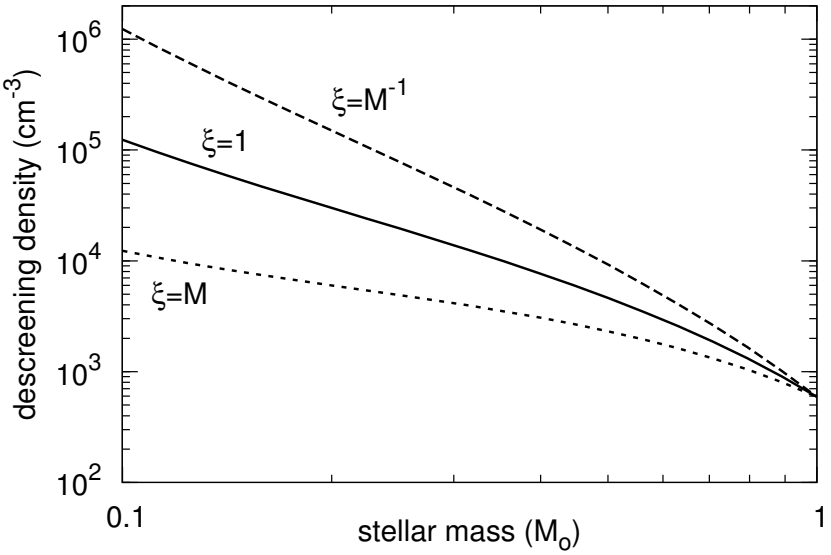

Figure 2: Critical interstellar density for descreening, defined as an event during which the astrosphere size is equal to the conventional liquid-water habitable-zone distance, as a function of parent-star mass in solar units. Three mass dependences of the stellar wind ram pressure are shown. Comparison with Fig. 1 shows that descreening densities are at or larger than the density above which gravitational focusing dominates. Even in the case in which low-mass stars have weaker winds ($\xi \propto M$), the descreening density still increases with decreasing mass, due to the severe dependence of the HZ distance on stellar mass.

A planetary system orbiting a star of mass 1 $M_\odot$ will be descreened if it encounters a region of density $\gtrsim 600\, V_{20}$ cm^{-3}. On the other hand a system orbiting a star of mass 0.2 $M_\odot$ must pass within a region of density $\gtrsim 10^4\, V_{20}$ cm^{-3} to be descreened, even if we assume no dependence of wind strength on mass or age. If we assume that the star-ISM velocity parameter, V_{20}, scales with the kinematic velocity dispersion, then V_{20} could be 2–3 times larger for both M stars (Fuchs et al., 2009) and older solar-type stars (Nordström et al., 2004) than for the Sun. Our results then imply that these stellar systems would require proportionally larger ISM densities to descreen the habitable zone. In this respect, our conclusions are somewhat conservative.

Section 3.3 will argue that such dense regions will be rarely encountered.

3.3 Frequency of Descreening as a Function of Stellar Mass

For any reasonable characterization of the ISM, the frequency of encounters of a planetary system with a cloud of a given density decreases with increasing density. Unfortunately this statement is difficult to quantify because interstellar densities are normally very poorly determined. The densities are almost always derived from the observed column density of some tracer (e.g. dust, or a molecule like CO), a conversion factor from tracer to to total column density, and then a conversion to density by dividing the column density by a characteristic size of the region of interest. This latter step is especially uncertain because the apparent size is determined by the sensitivity limit of the observations (column density normally decreases outward on average) and by the adopted distance to the region. However we can use the approach of Talbot and Newman (1977) as applied to various catalogues of regions identified as discrete "clouds" in different surveys in order to see that, even given these uncertainties and selection effects, the frequency of occurrence of dense ISM regions must decrease rapidly with increasing density.

Talbot and Newman (1977) used the Lynds (1962) catalogue of about 1800 "dark clouds,"* for which Lynds provided "opacity classes" and angular areas. Grouping these clouds into bins of a given column density range using the opacities, and using the mean size $R(N)$ for each group, gives the number of clouds with density in each density range. Plotted as a histogram, this gives the number of clouds per unit volume of space per unit density range, denoted $n_{\rm cl}(N)$, where N is the internal particle density. If $l(N)$ is the average number of clouds

*Regions on photographic plates that appear darker than the surrounding area because of reduction in the number of visible stars by dust extinction.

encountered of density $(N, N+dN)$ per unit line of sight distance, then $n_{\rm cl}(N) = [\pi R(N)^2\ l(N)]^{-1}$. Since the frequency of encounters is proportional to $l(N)^{-1}$, this gives a frequency $\nu \propto R(N)^2\ n_{\rm cl}(N)$.

We reexamined the cloud property table given by Talbot and Newman (1977), but we use only the data for the three highest opacity classes.† Using the derived average densities in each class, we find the distribution $n_{\rm cl}(N) \propto N^{-1.8}$ and $R(N) \propto N^{-0.8}$, giving a cumulative frequency of encounters $\nu(>N) \propto N^{-2.4}$. This agrees with the exponent of -2.3 obtained using directly the $l(>N)$ values in their table, or the scaling of their quantity N_e which is the number of expected encounters by the Sun over 4.6 Gyr.

This result is very uncertain because the Lynds cloud sample, besides its small size, suffers from a number of selection effects:

1. Clouds with angular sizes less than about 2–5 arcmin cannot be detected on Palomar Schmidt plates because the number of background stars is too small. This corresponds to a minimum detectable cloud size that increases with distance. Since smaller clouds tend to be denser, the density probability distribution is probably too flat because of this effect.

2. Column density detection is somewhat restrictive, because regions with extinction less than about one magnitude cannot be detected as a decrease in background star density, while at extinctions above about 5–6 magnitudes clouds look black independent of their extinction. The latter effect causes the catalogue to lump clouds of densities above the saturation threshold into the bin of highest column density, again making the apparent probability distribution of cloud densities appear too flat.

3. The increasing number of foreground stars makes it progressively more difficult to detect clouds farther than several hundred parsecs. This effect produces an underestimate of the extinction to distant large, and usually lower-density, clouds.

4. Nearby clouds likely obscure more distant clouds, so that some small clouds located in front of larger clouds are not detected, and so on (Scalo and Lazarian, 1996).

5. Distances to individual clouds detected in extinction are very uncertain. A way around this would be to examine only clouds in nearby complexes, like Taurus, which are all at about the same distance, but then the number of clouds would be small for statistical purposes (see Scalo, 1985). Talbot and Newman

†The points for "Standard cloud," actually derived from reddening statistics, "CO" and "HI" are ill-defined averages for entire surveys, and the lower opacity class extinction clouds suffer from selection effects as explained below and as can be seen in Fig. 1 of Talbot and Newman.

(1977) assumed they were all at the same distance.

For these reasons we have also derived the *relative* frequency of encounters with regions above a given density using the FCRAO Outer Galaxy Survey of carbon monoxide emission, which gives data for over 10,000 clouds (Heyer *et al*., 2001). This survey is subject to selection effects analogous to 1 (angular resolution limit) and 2 (CO can only be excited above a density of about 100 cm^{-3} but the [^{12}CO] line saturates at large column densities; also there is a sensitivity threshold on column density) above. The CO sample does not suffer from uncertainties 3–5 above because the clouds are detected using a spectral line, and the velocity information not only separates clouds along the same line of sight but allows distance estimates based on a kinematic model (rotation curve) for the Galaxy. We used the cloud properties from this survey (available electronically) to construct a density probability distribution $n_{\mathrm{cl}}(N)$, but chose to include only clouds with distances less than 5 kpc, since a plot of the number of clouds vs. distance indicated that incompleteness becomes serious beyond this point. We note that the clouds were identified by decomposition of larger structures, so the catalogue does not contain larger, and on average less dense, regions within which the catalogued clouds were contained (Heyer, private communication). This should not affect our results much because these larger regions have average densities that are mostly below the critical descreening density for any but the most massive parent stars considered here. Following Heyer *et al*., we take the calculated CO luminosity L_{CO} to be proportional to the mass of the cloud and then divide by the size cubed in order to estimate the average internal density. Following this procedure, we find that $n_{\mathrm{cl}}(N)$ declines rapidly with density. If a power law is fit to the histogram, excluding the highest and lowest bins, the cumulative probability distribution function at the high-density end (2×10^3 to 2×10^4 cm^{-3}) has a power-law slope of about -3, similar to the result found for the Lynds clouds. We also find the $R(N)\propto N^{-1}$ for this sample; this result is in part a reflection of the same selection effect as for the Lynds cloud sample, since the surveys tend to be restricted in column density, yielding such a correlation. Nevertheless we adopt it as an average correlation. This gives a density dependence of the cumulative encounter rate of N^{-4}, compared to $N^{-2.4}$ from Talbot and Newman. We also performed the same calculation but assuming all the clouds are at the same distance, to mimic the selection effect due to the unknown distances in Talbot and Newman's calculation, and find that $n_{\mathrm{cl}}(>N)$ becomes basically flat, but the distortion should be less severe for Talbot and Newman because the range in distances is smaller.

We can also estimate the *absolute* frequency of descreening events for solar-

mass stars from the Heyer *et al*. (2001) CO cloud catalogue and compare to Talbot and Newman's result for extinction clouds. For the 7900 CO clouds within 5 kpc, we estimate a volume surveyed of 0.86 kpc^3, assuming the clouds are distributed in a uniform disk with a half-thickness of 50 pc, which is close to most estimates for the scale height of the CO distribution perpendicular to the plane of the Galaxy. This yields the total cloud space density $n_{\rm cl}$. Most of these clouds are at average internal densities above 300 cm^{-3} (the number declines rapidly below this density, suggesting selection effects), which is roughly the estimated descreening density for the solar system (Fig. 2). The frequency of encounters is approximately $\nu = \pi \langle R^2 \rangle n_{\rm cl} \bar{v}$, where $\bar{v}$ is the mean star-cloud velocity (see Talbot and Newman, 1977).[‡] We find a mean square cloud radius $\langle R^2 \rangle = 1.2$ pc^2. Adopting a mean star-cloud velocity of 20 km s^{-1} gives a descreening frequency of 0.7 Gyr^{-1}. This is about six times smaller than obtained from including only the Lynds class 3–6 clouds from Talbot and Newman (1977, Table 1). Since we found that placing the Heyer *et al*. clouds all at the same distance significantly flattens the $n_{\rm cl}$ distribution, the assumption of a single distance could be part of the discrepancy. A major difference arises from the fact that the mean square sizes in the Lynds sample are much larger than found for the Heyer *et al*. sample. Such differences are perhaps expected because of the different selection criteria and selection effects (see Heyer *et al*. 2001 for discussion in the CO sample), and the different distances to which the surveys extend, but this expectation gives us no basis to decide which is the more realistic estimate. The difference should probably be considered a reflection of the inherent uncertainty involved in estimating the descreening frequency. Both results are lower limits because of the resolution effect discussed earlier, by which smaller, denser clouds are missed at larger distances, but we do not know the size of the corresponding correction factor.

Given these considerations, we think that the descreening frequency for the Sun cannot be estimated to better than an order of magnitude, but probably lies between 1 and 10 Gyr^{-1}. Since the critical descreening density scales approxi-

[‡]Our frequency estimates assume a random distribution of clouds, but aren't much changed by the fact that these clouds, as well as those in Lynds (1962) sample, are actually clustered into larger structures. The *mean* encounter frequency is roughly the volume filling fraction of the clouds divided by their radius, and neither of these quantities is affected by clustering as long as the clouds don't overlap. The time series of encounters will be radically different in the clustered case, with long periods without descreening punctuated by clusters of frequent descreenings, but the *average* rate of encounters is similar if taken over a sufficiently long time interval (~ 1 Gyr here). For recent history, however, this clustering effect would be important. We discuss the details of the time history during intrusion into a large complex using hydrodynamic simulations in a separate publication.

mately as M^{-2} (Eq. 16), and $n_{\rm cl}(>N)$ decreases rapidly with N, we see that the descreening frequency declines extremely rapidly with decreasing stellar mass. Using the dark cloud $n_{\rm cl}(>N)$ power-law slopes found above, we get a mass dependence of M^5, while the CO cloud slopes yield M^8.

It should be pointed out that these results only apply to relatively dense clouds that can be seen in extinction or CO, and we do not know how the frequency scales with density for smaller densities. In addition, our estimated rates for dense regions are probably underestimates, since both the Lynds and Heyer *et al*. (2001) cloud catalogues select against dense clouds because of resolution effects, as discussed above.

Since we showed earlier that an M star planet must encounter a region of density $\sim 1\times10^3$ cm^{-3} (for M0, $\sim 0.5M_\odot$) to 3×10^4 cm^{-3} (for M9, $\sim 0.1M_\odot$) for descreening, while a solar-type star requires only ~ 600 cm^{-3}, the frequency estimates given above imply that descreening will occur 10^2 to 10^9 times less frequently for M star planets (i.e., never). Even for somewhat higher mass stars, the frequency of descreening is apparently such a strongly decreasing function of density that, given the crude estimate of 1–10 descreening encounters per Gyr for the Earth, even stars of spectral types late G and early K should be relatively immune from descreening.

4 Summary and Conclusions

We have used a ram-pressure balance model for calculating the size of astrospheres in the apex direction around solar- and subsolar-mass stars to compute the minimum interstellar density required to "descreen" a planet in the habitable zone. We showed that gravitational focusing of incoming particle trajectories causes an enhancement of the ISM ram pressure and a consequent dependence of the astrosphere size on the parent-star mass when the local ISM density rises above $\sim 100\ M^{-2}$ cm^{-3}, where M is the stellar mass in solar units. We have included the effects of gravitational focusing in calculating the ISM densities required to descreen planets in the habitable zone of solar-like and lower-mass stars and find a critical descreening density of roughly $600\ M^{-2}$ cm^{-3}. Finally, we have estimated the frequency of descreening encounters as 1–10 Gyr^{-1} for solar-type stars and 10^2–10^9 times less frequent for M stars, so habitable planets around M stars will most likely never be exposed to the unfiltered ISM flow.

We caution that these results are sensitive to the parameters of the stellar winds of low-mass stars. Studies of mass-loss rates for M stars have not yet well con-

strained the dependence of the mass-loss rate on mass or age. Preliminary results (e.g. Wood *et al*., 2002, 2005) suggest that the wind strength may increase with decreasing age and mass, but examples to the contrary do exist. While we neglect the age dependence of the wind strength for this discussion, we do find that even a mass dependence in which the mass-loss rate is linearly dependent on the stellar mass does not change our results (see Fig. 2). Deeper surveys of stellar mass-loss rates as a function of mass and age would be beneficial to understanding the astrospheric environment around low-mass stars, which are potentially the most common sites for habitable planets in the Galaxy (Scalo *et al*., 2007).

Acknowledgements

This work was partially supported by the NASA Exobiology Program, Grant NNG04GK43G, and the NASA Astrobiology Institute, Virtual Planetary Laboratory Lead Team. D. Smith was supported by the NSF Graduate Student Research Fellowship and Harrington Doctoral Fellowship Programs.

References

Abramowitz, M., Stegun, I.A., Eds. (1972) *Handbook of Mathematical Functions*, Dover, NY.

Begelman, M.C. and Rees, M.J. (1976) Can cosmic clouds cause climatic catastrophes? *Nature*, 261, 298–299.

Bourke, T.L., Myers, P.C., Robinson, G., and Hyland, A.R. (2001) New OH Zeeman measurements of magnetic field strengths in molecular clouds. *Astrophys. J.*, 554, 916–932.

Bzowski, M., Fahr, H.J., and Rucinski, D. (1996) Interplanetary neutral particle fluxes influencing the Earth's atmosphere and the terrestrial environment. *Icarus*, 124, 209–219.

Crutcher, R.M. (1999) Magnetic fields in molecular clouds: observations confront theory. *Astrophys. J.*, 520, 706–713.

Danby, J.M.A. and Camm, G.L. (1957) Statistical dynamics and accretion. *Mon. Not. Roy. Astr. Soc.*, 117, 50–71.

Delfosse, X., Forveille, T., Segransan, D., Beuzit, J.-L., Udry, S., Perrier, C., and Mayor, M. (2000) Accurate masses of very low mass stars. IV. Improved mass-luminosity relations. *Astron. Astrophys.*, 364, 217–224.

Erkaev, N.V., Penz, T., Lammer, H., Lichtnegger, H.I.M., Wurz, P., Biernat, H.K., Griessmeier, J.-M., and Weiss, W.W. (2005) Plasma and magnetic field parameters in the vicinity of short periodic giant exoplanets. *Astrophys. J. Supp.*, 157, 396–401.

Fahr, H.J. (1968) On the influence of neutral interstellar matter on the upper atmosphere. *Astrophys. Sp. Sci.*, 2, 474–495.

Fahr, H.J., Kausch, T., and Schere, H. (2000) A 5-fluid hydrodynamic approach to model the solar system-interstellar medium interaction. *Astr. Astrophys.*, 357, 268–282.

Ferrière, K.M. (2001) The interstellar environment of our galaxy. *Rev. Mod. Phys.*, 73, 1031–1066.

Fite, W., Smith, A., and Stebbings, R. (1962) Charge transfer in collisions involving symmetric and asymmetric resonance. *Roy. Soc. London Proc. Ser. A*, 268, 527–536.

Florinski, V., Pogorelov, N.V., Zank, G.P., Wood, B.E. and Cox, D.P. (2004) On the possibility of a strong magnetic field in the local interstellar medium. *Astrophys. J.*, 604, 700–706.

Florinski, V., Zank, G.P., and Axford, W.I. (2003) The Solar System in a dense interstellar cloud: Implications for cosmic-ray fluxes at Earth and ^{10}Be records. *Geophys. Res. Lett.*, 30, 2206–2210.

Frisch, P. C., Slavin, J. D. 2006. The Sun's journey through the local interstellar medium: the paleoLISM and paleoheliosphere. *Astrophysics and Space Sciences Transactions*, 2, 53–61.

Fuchs, B., and 13 others. (2009) The kinematics of late-type stars in the solar cylinder studied with SDSS data. *Astron. J.*, 137, 4149–4159.

Grenfell, J.L., Griessmeier, J.-M., Patzer, B., Rauer, H., Segura, A., Stadelmann, A., Stracke, B., Titz, R., von Paris, P. (2006) Biomarker Response to Galactic Cosmic Ray Induced NO_x and the Methane Greenhouse Effect in the At-

mosphere of an Earthlike Planet Orbiting an M Dwarf Star. *Astrobiology*, 7, 208–220.

Griessmeier, J.-M., Stadelmann, A., Motschmann, U., Belivsheva, N.K., Lammer, H., Biernat, H.,K. (2005) Cosmic ray impact on Extrasolar Earth-like planets in close-in habitable zones. *Astrobiology*, 591, 1–12.

Henry, T.J., Franz, O.G., Wasserman, L.H., Benedict, G.F., Shelus, P.J., Ianna, P.A., Kirkpatrick, J.D., and McCarthy, D.W. (1999) The optical mass-luminosity relation at the end of the main sequence (0.08–0.20 $M_{\odot}$). *Astrophys. J.*, 512, 864–873.

Heyer, M.H., Carpenter, J.M., and Snell, R.L. (2001) The equilibrium state of molecular regions in the outer Galaxy. *Astrophys. J.*, 551, 852–866.

Hillenbrand, L.A. and White, R.J. (2004) An assessment of dynamical mass constraints on pre-main-sequence evolutionary tracks. *Astrophys. J.*, 604, 741–757.

Kasting, J.F., Whitmire, D.P., and Reynolds, R.T. (1993) Habitable zones around main sequence stars. *Icarus*, 101, 108–128.

Khodachenko, M.L., and 10 others. (2006) Coronal Mass Ejection (CME) Activity of Low Mass M Stars as an Important Factor for the Habitability of Terrestrial Exoplanets. I. CME Impact on Expected Magnetospheres of Earth-like Exoplanets in Close-in Habitable Zones. *Astrobiology*, 7, 167–184.

Larson, R.B. (1981) Turbulence and star formation in molecular clouds. *Mon. Not. Roy. Astr. Soc.*, 194, 809–826.

Lynds, B.T. (1962) Catalogue of dark nebulae. *Astrophys. J. Supp.*, 7, 1–60.

McCrea, W.H. (1975) Ice ages and the Galaxy. *Nature*, 255, 607–609.

McKay, C.P. (1985) Noctilucent cloud formation and the effects of water vapor variability on temperatures in the middle atmosphere. *Planet. Space Sci.*, 33. 761–771

McKay, C.P. and Thomas, G.E. (1978) Consequences of a past encounter of the Earth with an interstellar cloud. *Geophys. Res. Lett.*, 5. 215–218.

Müller, H.-R., Frisch, P. C., Florinski, V., Zank, G. P. 2006. Heliospheric Response to Different Possible Interstellar Environments. *Astrophys. J.*, 647, 1491–1505.

Müller, H.-R., Frisch, P. C., Fields, B. D., and Zank, G. P. (2008) The Heliosphere in Time. Sp. Sci. Rev., 163.

Nordström, B., Mayor, M., Andersen, J., Holmberg, J., Pont, F., Jørgensen, B.R., Olsen, E.H., Udry, S., and Mowlavi, N. (2004) Ages, metallicities, and kinematic properties of $\sim$ 14,000 F and G dwarfs. *Astr. Astrophys.*, 418, 989–1019.

Parker, E.N. (1963) *Interplanetary dynamical processes*, Wiley, NY, pp. 113–128.

Pavlov, A.A., Pavlov, A.K., Mills, M.J., Ostryakov, V.M., Vasilyev, G.I., and Toon, O.B. (2005a) Catastrophic ozone loss during passage of the Solar system through an interstellar cloud. *Geophys. Res. Lett.*, 32, L01815–L01818.

Pavlov, A.A., Toon, O.B., Pavlov, A.K., Bally, J., and Pollard, D. (2005b) Passing through a giant molecular cloud: "Snowball" glaciations produced by interstellar dust. *Geophys. Res. Lett.*, 32, L03705–L03708.

Penz, T., and Micela, G. (2008) X-ray induced mass loss effects on exoplanets orbiting dM stars. *Astr. Astrophys.*, 479, 579–584.

Preusse, S., Kopp, A., Büchner, J., and Motschmann, U. (2005) Stellar wind regimes of close-in extrasolar planets. *Astron. Astrophys.*, 434, 1191–1200.

Scalo, J.M. (1985) *Fragmentation and hierarchical structure in the interstellar medium.* In *Protostars and Planets II*, ed. D.C. Black and M.S. Matthews, Univ. Ariz. Press, pp. 201–296.

Scalo, J.M., and 14 others. (2007) M Stars as Targets for Terrestrial Exoplanet Searches and Biosignature Detection. *Astrobiology*, 7, 85–166.

Scalo, J.M. and Lazarian, A. (1996) Occlusion effects and the distribution of interstellar cloud sizes and masses. *Astrophys. J.*, 469, 189–193.

Scherer, K., Fichtner, H., and Stawicki, O. (2002) Shielded by the wind: the influence of the interstellar medium on the environment of the Earth. *J. Atmospher. Solar-Terr. Phys.*, 64, 795–804.

Smith, E.J., Marsden, R.G., and 10 others. (2003) The sun and heliosphere at solar maximum. *Science*, 302, 1165–1169.

Stone, E.C., Cummings, A.C., McDonald, F.B., Heikkila, B.C., Lal, N., Webber, W.R. (2005) Voyager 1 explores the termination shock region and the heliosheath beyond. *Science*, 309, 2017–2020.

Talbot, R.J. and Newman, M.J. (1977) Encounters between stars and dense interstellar clouds. *Astrophys. J. Supp.*, 34, 295–308.

Talbot, R.J., Butler, D.M., and Newman, M.J. (1976) Climatic effects during passage of the Solar System through interstellar clouds. *Nature*, 262, 561–562.

Tarter, J.C., and 31 others. (2007) A Reppraisal of the Habitability of Planets around M Dwarf Stars. *Astrobiology*, 7, 30–65.

Whang, Y.C., Burlaga, L.F., Wang, Y.-M., and Sheeley, N.R. (2003) Solar wind speed and temperature outside 10 AU and the termination shock. *Astrophys. J.*, 589, 635–643.

Wimmer-Schweingruber, R.F. and Bochsler, P. (2000) Is there a record of interstellar pick-up ions in lunar regolith? In *Acceleration and Transport of Energetic Particles Observed in the Heliosphere: AIP Conf. Proc.*, edited by R.A. Mewaldt *et al.*, Melville, NY, pp. 270–273.

Wimmer-Schweingruber, R.F. and Bochsler, P. (2001) A non-solar origin of the "SEP" component in lunar soils. In *The Outer Heliosphere: The Next Frontiers, COSPAR Colloquia Ser. 11*, edited by K. Scherer, H. Fichtner, H.J. Fahr, and E. Marsch, Pergamon Press, Amsterdam, pp. 507–510.

Witte, M. (2004) Kinetic parameters of interstellar neutral helium: Review of results obtained during one solar cycle with the Ulysses/GAS-instrument. *Astron. Astrophys.*, 426, 835–844.

Wood, B.E., Müller, H.-R., Zank, G.P., and Linsky, J.L. (2002) Measured mass-loss rates of solar-like stars as a function of age and activity. *Astrophys. J.*, 574, 412–425.

Wood, B.E., Müller, H.-R., Zank, G.P., Linsky, J.L., and Redfield, S. (2005) New Mass-Loss Measurements from Astrospheric Lyα Absorption. *Astrophys. J.*, 628, L143–L146.

Yabushita, S. and Allen, A.J. (1989) On the effect of accreted interstellar matter on the terrestrial environment. *Mon. Not. Roy. Astr. Soc.*, 238, 1465–1478.

Yeghikyan, A. and Fahr, H. (2004a) Effects induced by the passage of the Sun through dense molecular clouds. I. Flow outside of the compressed heliosphere. *Astr. Astrophys.*, 415, 763–770.

Yeghikyan, A. and Fahr, H. (2004b) Terrestrial atmospheric effects induced by counterstreaming dense interstellar cloud material. *Astr. Astrophys.*, 425, 1113–1118.

Zank, G.P. (1999) Interaction of the solar wind with the local interstellar medium: A theoretical perspective. *Sp. Sci. Rev.*, 89, 412–688.

Zank, G.P. and Frisch, P.C. (1999) Consequences of a change in the Galactic environment of the Sun. *Astrophys. J.*, 518, 965–973.

Zank, G. P., Müller, H.-R., Florinski, V., Frisch, P. C. 2006. Heliospheric Variation in Response to Changing Interstellar Environments. Solar Journey: The Significance of our Galactic Environment for the Heliosphere and Earth 338, 23.